
This is an electronic reprint of the original article.
This reprint may differ from the original in pagination and typographic detail.

Riuttanen, Lauri; Kivisaari, Pyry; Svensk, Olli; Oksanen, Jani; Suihkonen, Sami
Electrical injection to contactless near-surface InGaN quantum well

Published in:
Applied Physics Letters

DOI:
[10.1063/1.4928248](https://doi.org/10.1063/1.4928248)

Published: 03/08/2015

Document Version
Publisher's PDF, also known as Version of record

Please cite the original version:
Riuttanen, L., Kivisaari, P., Svensk, O., Oksanen, J., & Suihkonen, S. (2015). Electrical injection to contactless near-surface InGaN quantum well. *Applied Physics Letters*, 107(5), Article 051106.
<https://doi.org/10.1063/1.4928248>

This material is protected by copyright and other intellectual property rights, and duplication or sale of all or part of any of the repository collections is not permitted, except that material may be duplicated by you for your research use or educational purposes in electronic or print form. You must obtain permission for any other use. Electronic or print copies may not be offered, whether for sale or otherwise to anyone who is not an authorised user.

Electrical injection to contactless near-surface InGaN quantum well

L. Riuttanen, P. Kivisaari, O. Svensk, J. Oksanen, and S. Suihkonen

Citation: *Appl. Phys. Lett.* **107**, 051106 (2015); doi: 10.1063/1.4928248

View online: <https://doi.org/10.1063/1.4928248>

View Table of Contents: <http://aip.scitation.org/toc/apl/107/5>

Published by the [American Institute of Physics](#)

Articles you may be interested in

[Diffusion injected multi-quantum well light-emitting diode structure](#)

Applied Physics Letters **104**, 081102 (2014); 10.1063/1.4866343

[Current injection to free-standing III-N nanowires by bipolar diffusion](#)

Applied Physics Letters **103**, 031103 (2013); 10.1063/1.4813754

[Thermophotonic heat pump—a theoretical model and numerical simulations](#)

Journal of Applied Physics **107**, 093106 (2010); 10.1063/1.3419716

[Ultimate limit and temperature dependency of light-emitting diode efficiency](#)

Journal of Applied Physics **105**, 093119 (2009); 10.1063/1.3125514

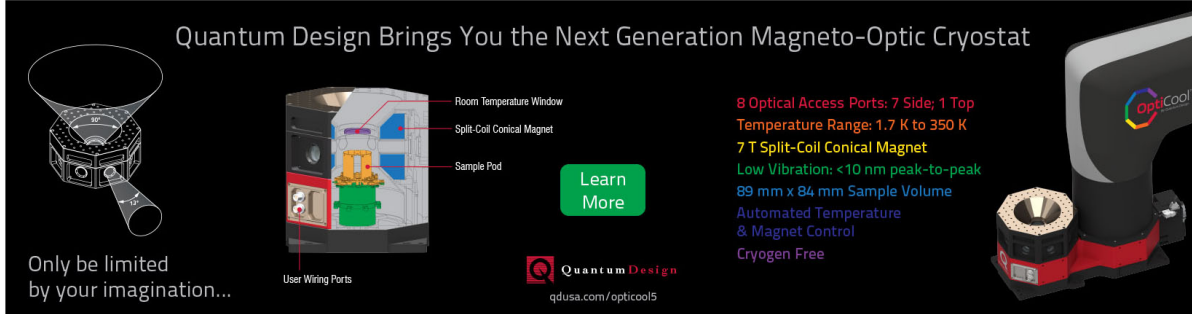
[On the correlation of the Auger generated hot electron emission and efficiency droop in III-N light-emitting diodes](#)

Applied Physics Letters **105**, 091106 (2014); 10.1063/1.4894862

[Effects of lateral current injection in GaN multi-quantum well light-emitting diodes](#)

Journal of Applied Physics **111**, 103120 (2012); 10.1063/1.4720584

Quantum Design Brings You the Next Generation Magneto-Optic Cryostat



Only be limited by your imagination...

Room Temperature Window
Split-Coil Conical Magnet
Sample Pod
User Wiring Ports

Learn More

Quantum Design
qdusa.com/opticool5

8 Optical Access Ports: 7 Side; 1 Top
Temperature Range: 1.7 K to 350 K
7 T Split-Coil Conical Magnet
Low Vibration: <10 nm peak-to-peak
89 mm x 84 mm Sample Volume
Automated Temperature & Magnet Control
Cryogen Free

Electrical injection to contactless near-surface InGaN quantum well

L. Riuttanen,^{1,a)} P. Kivisaari,² O. Svensk,¹ J. Oksanen,² and S. Suihkonen¹

¹Department of Micro- and Nanosciences, Aalto University, P.O. Box 13500, FI-00076 Aalto, Finland

²Department of Biomedical Engineering and Computational Science, Aalto University, P.O. Box 12200, FI-00076 Aalto, Finland

(Received 22 May 2015; accepted 28 July 2015; published online 5 August 2015)

Charge injection to the prevailing and emerging light-emitting devices is almost exclusively based on the double heterojunction (DHJ) structures that have remained essentially unchanged for decades. In this letter, we report the excitation of a near surface indium gallium nitride (InGaN) quantum well (QW) by bipolar carrier diffusion from a nearby electrically excited pn-homojunction. The demonstrated near surface QW emitter is covered only by a 10 nm GaN capping leaving the light-emitting mesa perfectly free of metals, other contact, or current spreading structures. The presented proof-of-principle structure, operating approximately with a quantum efficiency of one fifth of a conventional single QW reference structure, provides conclusive evidence of the feasibility of using diffusion injection to excite near surface light-emitting structures needed, e.g., for developing light emitters or photo-voltaic devices based on nanoplasmonics or free-standing nanowires. In contrast to the existing DHJ solutions or optical pumping, our approach allows exciting nanostructures without the need of forming a DHJ, absorbing layers or even electrical contacts on the device surface. © 2015 AIP Publishing LLC. [<http://dx.doi.org/10.1063/1.4928248>]

Practically all modern inorganic light-emitting diode (LED) designs are based on double heterojunctions (DHJs) whose structure and current injection principle have remained essentially unchanged for decades. The conventional DHJ design does not, however, adapt well to current injection to nanostructured active regions (ARs) located close to device surfaces due to challenges, e.g., in fabricating nanostructured DHJs¹ and the formation of leakage current inducing depletion layers.² This slows down the research and development of emerging optoelectronic nanodevices such as photonic crystal,³ surface plasmon enhanced,^{2,4-8} nanowire (NW),^{1,9,10} and quantum-dot (QD)¹¹ structures.

In a conventional DHJ, the minority carrier diffusion may extend over relatively long distances even in the presence of the DHJ potential barriers.^{12,13} Here, we show that a fundamentally different approach based on charge diffusion enables electrical excitation of surface light emitting materials without using a DHJ, absorbing layers or even electrical contacts on the device surface. Instead, the diffusion based emitter fully separates the AR from the pn-junction, located within the diffusion length from the AR. In such a structure the AR acts as a carrier drain inducing a bipolar diffusion current into the AR. Using the diffusion injection (DI)-scheme, emitters based on, e.g., near surface quantum wells (QWs), surface NWs, QDs, and layered 2D emitting materials can be fabricated without top contacts. This will allow integration of nano-scale surface light emitters in applications where DHJs cannot be used.

In this letter, we demonstrate the DI-excitation for near surface light-emitting structures by electrically exciting an indium gallium nitride (InGaN) QW located on top of a GaN pn-homojunction. The demonstrated surface LED (S-LED) is illustrated in Figure 1(a). The QW is covered only by a

10 nm GaN capping leaving the light-emitting surface perfectly free of metals or other contact structures. In contrast to the previously demonstrated buried multi-quantum well (MQW) diffusion injected structures,^{14,15} where the possibility of current transport through the semi-insulating buffer layer could not be completely ruled out, the S-LED clearly

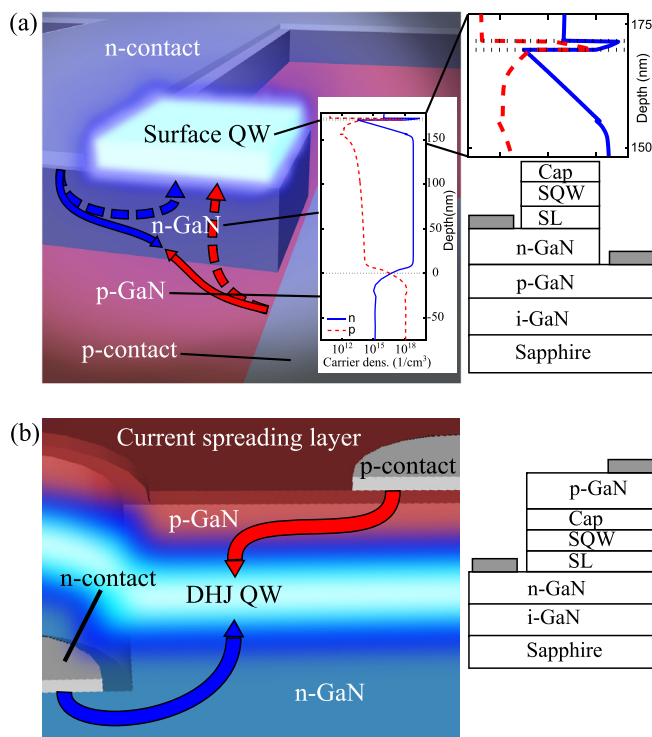


FIG. 1. (a) The S-LED structure illustrating the drift (solid line) and diffusion (dashed line) current components for electrons (blue) and holes (red) and electron and hole densities in the device under operation. (b) The conventional DHJ structure showing the drift current components of electrons (blue) and holes (red).

^{a)}Electronic mail: lauri.riuttanen@aalto.fi

shows that the QW is excited by carrier diffusion through the bottom interface of the QW only. As the first demonstration of an electrically injected near surface QW, the S-LED provides conclusive evidence of its feasibility for exciting surface nanostructures. Simulations additionally suggest that with further development near surface QW emitters can achieve near unity injection efficiency.¹⁶ This clearly highlights the potential of DI in developing electrically injected surface nanostructures for, e.g., light emitters or photovoltaic devices based on nanoplasmonics or free-standing contactless light-emitting or photovoltaic nanowires.

The operation of the studied proof-of-principle S-LED is based on the bipolar diffusion of charge carriers from the electrically excited pn-homojunction to the near surface QW as indicated by the arrows in Figure 1(a). This is in stark contrast with conventional DHJ structures where charge transport takes place through separate surfaces interfacing to the n- and p-type materials, as illustrated in Figure 1(b). When the S-LED is biased, the pn-junction becomes excited, as in conventional LEDs. However, for moderate excitations the recombination at the pn-junction remains small in comparison to charge carrier diffusion toward the QW that provides a strong recombination channel. The electron and hole densities in the S-LED under forward bias, also illustrated in Figure 1(a), are both large only in the QW region. Since the radiative recombination becomes strong only for large electron and hole densities and the minority carrier density in the other layers is modest, practically no light emission takes place outside the QW.

The light emission from the S-LED is made possible by functionally separating the pn-junction initially creating the excitation and the near surface QW where the radiative recombination takes place. In suitably engineered structures, the carriers injected into the p- and n-layers are efficiently transported to the near surface QW by bipolar diffusion through the bottom interface of the QW. Therefore, there is no carrier flux through the top interface of the QW and the net current through any horizontal cross-section of the QW is always zero as in optical pumping. However, in contrast to direct optical pumping, the demonstrated electrical excitation method does not directly generate carriers in the surface quantum well.

The S-LED and a single QW reference LED structures were fabricated on c-plane sapphire substrates using metal organic vapor phase epitaxy (MOVPE). Both devices included a 3 μm thick unintentionally doped GaN (i-GaN) buffer layer. The fabricated S-LED additionally consisted of a 1.3 μm p-GaN layer followed by a 150 nm n-doped layer, a 16 nm unintentionally doped InGaN/GaN superlattice (SL) underneath layer,¹⁷ and a 2 nm InGaN QW and a 10 nm i-GaN capping layers. The carrier concentrations of the layers at room temperature were $2 \times 10^{17}/\text{cm}^3$, $5 \times 10^{18}/\text{cm}^3$, and $5 \times 10^{16}/\text{cm}^3$ for p-GaN, n-GaN, and i-GaN, respectively. The p-GaN layer was grown using hydrogen as carrier gas in order to reduce the surface roughness of the p-GaN layer.¹⁸ The reference LED consisted of a 700 nm n-GaN followed by the underneath InGaN/GaN SL, the QW, a p-doped electron blocking layer (EBL) SL consisting of 9 pairs of 2 nm AlGaIn and GaN layers and 300 nm of p-doped GaN.

Following the MOVPE growth, the wafers were patterned with standard lithography techniques. The mesa structures for the QW and n-contact were etched in two subsequential etching steps. In the first step, the wafer was etched to reveal the n-GaN layer outside the small emitter mesa region consisting of the 10 nm GaN capping, QW, and the InGaN/GaN SL. In the second step, the wafer was etched to reveal the p-GaN layer outside the emitter mesa and the n-contact regions, leaving a 2 μm distance between the QW mesa and the n-contact mesa. Etching was performed using inductively coupled plasma reactive ion etching (ICP-RIE). The emitter mesa was shaped as a 30 $\mu\text{m} \times 30 \mu\text{m}$ square and the n- and p-layers were contacted with Ti/Al and Ni/ITO layers also leaving a 2 μm gap to the edges of the n-GaN mesa and the emitter mesa. The contact pads were designed as large squares reaching to the emitter mesa through narrow extensions. Schematic illustration of the processed device is shown in Figure 1(a). After processing, the wafer was diced and the samples were attached to a heat sink. The reference LED was processed to chips with surface area of 500 $\mu\text{m} \times 500 \mu\text{m}$. A transparent Ni/Au current spreading layer was deposited on the p-GaN. Ti/Au was used for the contact pad metalizations.

Under electrical injection using probe needles, a bright blue emission from the 30 \times 30 μm^2 S-LED was observed. Figures 2(a)–2(d) show the microscope images of the S-LED under various injection currents. Figures 2(e) and 2(f) also show the emission intensity profiles along X and Y directions as defined in Figure 2(a). The intense light emission from the S-LED and the absence of any band-to-band UV emission from the GaN layers clearly indicate that the charge carriers are transported to the QW through its bottom interface by diffusion. At low injection currents, the emission is strongest near the n-type contacts due to the resistive losses of the 150 nm thick n-layer being larger than in the much thicker p-type layer, resulting in a faster decay of the quasi-Fermi level of electrons in the lateral direction. At larger injection currents, the emission becomes more uniform due to the interplay between the resistive losses in the n- and p-type layers, and the associated nonuniform current spreading to the QW. In addition, the emission is slightly stronger on the bottom of the structure located closest to the p-contact, which suggests that the stronger emission could be due to the smallest resistive hole transport losses and, to smaller extent, due to variations in the QW compositions observed in microphotoluminescence ($\mu\text{-PL}$) measurements performed with 405 nm laser excitation prior to the deposition of the electrical contacts. Due to etching damage on the p-GaN surface the bias voltages in the S-LED generally exceeded 10 V and the voltage drop at the contacts dominated the current-voltage (I-V) characteristics, making it uninformative for analyzing the device performance. However, according to simulations and previous studies,^{14,15} it is expected that the I-V characteristics of the device itself do not differ significantly from conventional DHJ structures. The large contact resistance also resulted in significant Joule heating leading to relatively high local operating temperatures.

The emission spectrum of the S-LED, shown in Figure 3, was measured using an electroluminescent setup on the emitter mesa side and averaged over the whole mesa. The

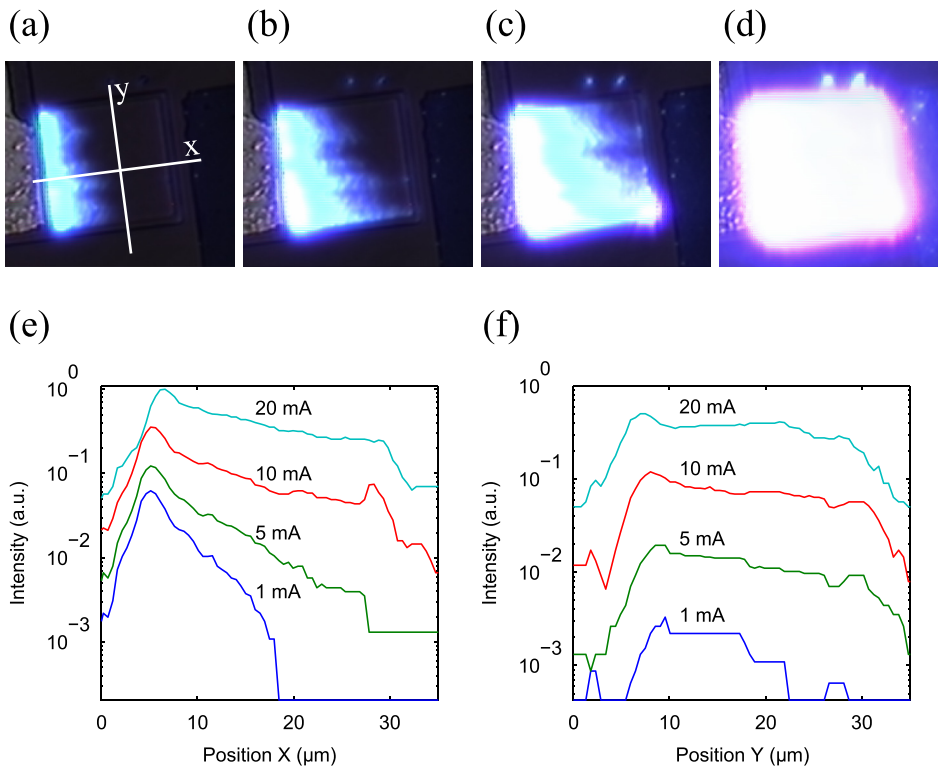


FIG. 2. Microscope images of the $30 \times 30 \mu\text{m}^2$ S-LED under electrical excitation with injection currents of (a) 1 mA, (b) 5 mA, (c) 10 mA, and (d) 20 mA. (e) and (f) Emission intensity profile along x and y directions defined in (a). With low injection, the QW emits mostly near the n-contact. By increasing the injection current, the emission becomes more uniform.

spectrum peaks at 460 nm, which corresponds to the band-to-band emission from the InGaN QW. No yellow band luminescence, often related to defects and vacancies in i-GaN or n-GaN,^{19–24} or 360 nm luminescence from the pn-homojunction was observed, indicating negligible amount of radiative recombination at the n-GaN layer and efficient carrier injection into the near surface QW. The absence of GaN band-to-band emission excludes the possibility of the optical excitation of the near surface QW by the pn-junction. The clearly visible oscillations in the spectrum match with the interference pattern expected from cavity formed by the substrate/GaN and GaN/air interfaces.

The optical output power of the S-LED is shown in the inset of Figure 3. The output power was measured indirectly using the larger reference LED as a comparison. First, the optical power of the reference LED was measured from the back side using an integrating sphere. Then, its surface brightness was measured using a microscope camera from the top and the brightness was normalized to correspond to the emission power density. Finally, the power density of the S-LED was estimated by comparing the surface brightness

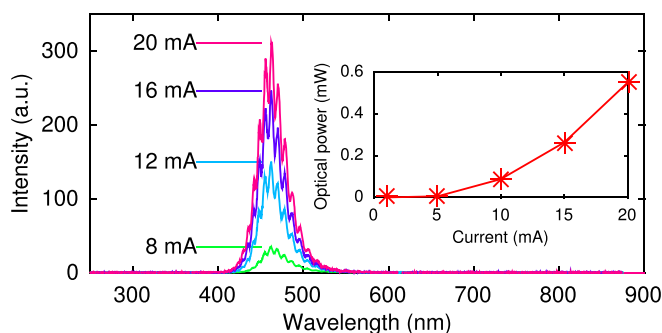


FIG. 3. Emission spectrum and the optical output power measured from the front side of the device.

from the microscope image of S-LED to the brightness of the reference LED. The optical power of the S-LED increases superlinearly as a function of the injection current. The superlinear behavior is due to conventional radiative vs. nonradiative recombination dynamics as well as increased operating temperature, which improves the hole injection into the QW.¹⁵ The efficiency of the S-LED is mainly limited by the modest injection efficiency originating from the unoptimized structure. Comparison of the S-LED and the reference LED shows that at an operating current of 20 mA the external quantum efficiency (EQE) of the S-LED reaches approximately 20% of the reference LED. At 20 mA injection current, the reference LED has reached its maximum EQE, while the S-LED EQE is still increasing. However, due to the differences between S-LED and the reference LED this should be considered an order of magnitude approximation.

Operation of the S-LED structure was also simulated with a standard semiconductor transport model consisting of the drift-diffusion equations, Poisson's equation, and the conventional carrier density-dependent models for radiative and nonradiative recombination.²⁵ The simulations were run for a temperature of 400 K to accommodate for the resistive heating of the S-LED, and the ionized doping densities were correspondingly set to $N_a = 1.2 \times 10^{18}/\text{cm}^3$ and $N_d = 6.1 \times 10^{18}/\text{cm}^3$. Other material parameters are similar to our previous publication.¹⁴ To simplify the modeling, the simulations were performed for a two dimensional structure essentially corresponding to the 2D cross section along the z-x plane in Figure 2(a) and assuming translational invariance in y-direction. With this choice, the simulations involved the most important lateral charge transfer effects as well as the diffusive current transport to the surface QW while keeping the simulations sufficiently uncomplicated.

Figure 4 shows the simulated band diagram of the S-LED through a straight vertical line at the center of the

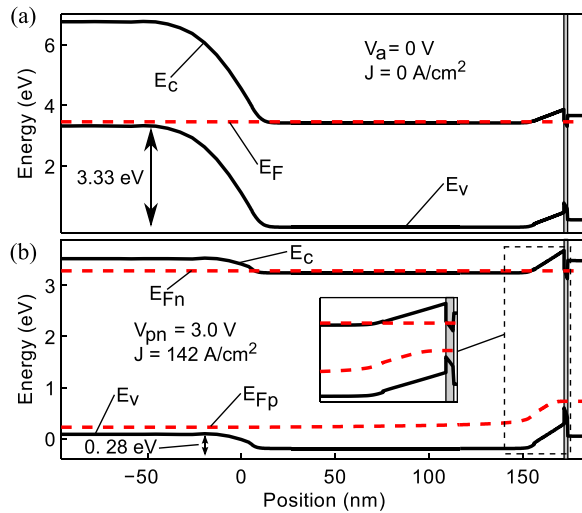


FIG. 4. Simulated conduction band E_c , valence band E_v , Fermi level E_F , quasi-Fermi levels for holes E_{Fp} and electrons E_{Fn} , and potential barrier heights of the S-LED (a) at zero bias and (b) at a bias voltage 3.6 V corresponding to an effective excitation voltage of 3.0 V at the pn-junction and a current density of 142 A/cm². The band diagrams are plotted through a straight vertical line at the center of the mesa starting from the p-type GaN and ending at the top of the GaN capping layer, and the QW is marked with a gray background.

QW mesa starting from the p-type GaN and ending at the top of the GaN capping layer. The band diagram in Figure 4(a) corresponds to zero bias while Figure 4(b) shows the band diagram under electrical excitation. In the equilibrium conditions of Figure 4(a), the large n-type doping next to the nominally undoped QW results in a large modulation doping as evidenced by the Fermi-level located close to the conduction band edge of the InGaN QW.

Figure 4(b) shows the band diagram under a bias voltage of 3.6 V and current density of 142 A/cm², resulting in an effective pn-junction bias of 3.0 V due to the high current density and associated resistive losses in the current spreading layers. The slightly increased pn-junction voltage is expected to include a substantial artificial contribution from the drift-diffusion simulations, which typically overestimates the hole transport losses.²⁶ The below band-gap effective bias of the pn-junction in the simulations shows that essentially no GaN band-to-band luminescence is expected to take place, as also shown by the measured spectrum in Figure 3. Instead, the excitation of the QW is enabled by diffusion of holes through the n-type GaN in to the lower band gap InGaN QW. Despite the relatively modest overall efficiency of the demonstrated S-LED, further simulations suggest that the efficiency can be significantly enhanced by using laterally doped miniaturized periodic structures and by optimizing the layer thicknesses, doping levels, lateral contact dimensions and the device geometry in general. For instance, optimizing the donor doping level in the n-GaN layer should increase the hole diffusion current significantly, while maintaining reasonable conductivity in the n-GaN layer. Furthermore, near unity injection efficiencies have been predicted for optimized diffusion injected surface nanowire light-emitters.¹⁶ The diffusion injection concept has also been shown to allow excitation of MQW structures.²⁷ The range of potential applications of the diffusion driven devices

covers, therefore, several fields ranging from the presently elusive light-emitters integrated on silicon to ubiquitous solid-state lighting applications with a wider choice of materials and emission wavelengths. The key benefit the S-LEDs can offer over the DHJ LEDs is the “contactless” current injection scheme—which may enable harnessing many previously impractical device structures—that can provide access to many performance boosting effects ranging from micro-concentration effects to plasmonic near-field enhancements.

In conclusion, we provide a conclusive experimental demonstration that bipolar diffusion can transport both electrons and holes into an active region located on the surface of a semiconductor device. The optical performance of the demonstrated S-LED is very promising as the optical power density of the studied proof-of-principle structure is of the same order as in the conventional single QW reference LED and its EQE is approximately one fifth of the reference LED. The S-LED exhibits several fundamental differences to conventional DHJ LEDs or optically pumped structures because (1) it provides a truly single sided electrical injection scheme enabling electrical excitation of ARs located at or near device surfaces, (2) it enables designing plasmonic and free standing nanowire devices that do not include top contacts, and (3) it allows optical pumping -like electrical excitation without direct generation of electron-hole pairs in the AR. With further optimization, the S-LED can therefore challenge the conventional current injection schemes in enabling various surface emitting structures. Since the diffusion injection approach is not limited to thin film QWs or III-nitrides, it can also be applied to other materials like conventional III-V compound semiconductors and silicon as well as to structures including contactless nanowires, plasmonic nanoparticles, functionalized surfaces, or even light emitting particles deposited from colloidal solutions. Therefore, the reported demonstration is considered to offer enormous potential for further development and for opening unexplored horizons for electrically injected structures that cannot be realized using conventional DHJ current injection or even optical pumping.

The authors thank the Aalto Energy Efficiency (AEF) programme, the Academy of Finland, The Nokia Foundation and the National Doctoral Programme in Nanoscience (NGS-NANO).

- ¹J. Wallentin, N. Anttu, D. Asoli, M. Huffman, I. Åberg, M. H. Magnusson, G. Siefert, P. Fuss-Kailuweit, F. Dimroth, B. Witzigmann, H. Q. Xu, L. Samuelson, K. Deppert, and M. T. Borgström, *Science* **339**, 1057 (2013).
- ²M.-K. Kwon, J.-Y. Kim, B.-H. Kim, I.-K. Park, C.-Y. Cho, C. C. Byeon, and S.-J. Park, *Adv. Mater.* **20**, 1253 (2008).
- ³J. J. Wierer, A. David, and M. M. Megens, *Nat. Photonics* **3**, 163 (2009).
- ⁴V. J. Sorger and X. Zhang, *Science* **333**, 709 (2011).
- ⁵R. F. Oulton, V. J. Sorger, T. Zentgraf, R.-M. Ma, C. Gladden, L. Dai, G. Bartal, and X. Zhang, *Nature* **461**, 629 (2009).
- ⁶D.-M. Yeh, C.-F. Huang, C.-Y. Chen, Y.-C. Lu, and C. C. Yang, *Nanotechnology* **19**, 345201 (2008).
- ⁷K. Okamoto, I. Niki, A. Shvartser, Y. Narukawa, T. Mukai, and A. Scherer, *Nat. Mater.* **3**, 601 (2004).
- ⁸W. L. Barnes, A. Dereux, and T. W. Ebbesen, *Nature* **424**, 824 (2003).
- ⁹D. Bayerl and E. Kioupakis, *Nano Lett.* **14**, 3709 (2014).
- ¹⁰L. Cao, J. S. White, J.-S. Park, J. A. Schuller, B. M. Clemens, and M. L. Brongersma, *Nat. Mater.* **8**, 643 (2009).

- ¹¹Y. Shirasaki, G. J. Supran, M. G. Bawendi, and V. Bulović, *Nat. Photonics* **7**, 13 (2013).
- ¹²K. J. Vampola, M. Iza, S. Keller, S. P. DenBaars, and S. Nakamura, *Appl. Phys. Lett.* **94**, 061116 (2009).
- ¹³H.-S. Kim, E. Brueckner, J. Song, Y. Li, S. Kim, C. Lu, J. Sulkin, K. Choquette, Y. Huang, R. G. Nuzzo, and J. A. Rogers, *Proc. Natl. Acad. Sci. U.S.A.* **108**, 10072 (2011).
- ¹⁴L. Riuttanen, P. Kivisaari, H. Nykänen, O. Svensk, S. Suihkonen, J. Oksanen, J. Tulkki, and M. Sopanen, *Appl. Phys. Lett.* **104**, 081102 (2014).
- ¹⁵L. Riuttanen, P. Kivisaari, O. Svensk, J. Oksanen, and S. Suihkonen, *IEEE Trans. Electron Devices* **62**, 902 (2015).
- ¹⁶P. Kivisaari, J. Oksanen, and J. Tulkki, *Appl. Phys. Lett.* **103**, 031103 (2013).
- ¹⁷P. Törmä, O. Svensk, M. Ali, S. Suihkonen, M. Sopanen, M. Odnoblyudov, and V. Bougrov, *J. Cryst. Growth* **310**, 5162 (2008).
- ¹⁸O. Svensk, S. Suihkonen, T. Lang, H. Lipsanen, M. Sopanen, M. Odnoblyudov, and V. Bougrov, *J. Cryst. Growth* **298**, 811 (2007).
- ¹⁹I.-H. Lee, I.-H. Choi, C. R. Lee, and S. K. Noh, *Appl. Phys. Lett.* **71**, 1359 (1997).
- ²⁰S. Li, C. Mo, L. Wang, C. Xiong, X. Peng, F. Jiang, Z. Deng, and D. Gong, *J. Lumin.* **93**, 321 (2001).
- ²¹M. A. Reshchikov and H. Morkoç, *J. Appl. Phys.* **97**, 061301 (2005).
- ²²J. L. Lyons, A. Janotti, and C. G. V. de Walle, *Appl. Phys. Lett.* **97**, 152108 (2010).
- ²³A. Kakanova-Georgieva, U. Forsberg, and E. Janzén, *Phys. Status Solidi A* **208**, 2182 (2011).
- ²⁴F. J. Xu, B. Shen, L. Lu, Z. L. Miao, J. Song, Z. J. Yang, G. Y. Zhang, X. P. Hao, B. Y. Wang, X. Q. Shen, and H. Okumura, *J. Appl. Phys.* **107**, 023528 (2010).
- ²⁵P. Kivisaari, J. Oksanen, and J. Tulkki, *J. Appl. Phys.* **111**, 103120 (2012).
- ²⁶Z. M. Simon Li, *J. Comput. Electron.* **14**, 409 (2015).
- ²⁷L. Riuttanen, P. Kivisaari, O. Svensk, T. Vasara, P. Myllys, J. Oksanen, and S. Suihkonen, *Proc. SPIE* **9363**, 93632A (2015).